

## THE GALACTIC OPEN CLUSTER NGC 6531 (M21)

BYEONG-GON PARK<sup>1</sup>, HWANKYUNG SUNG<sup>2</sup>, AND YONG HEE KANG<sup>3</sup><sup>1</sup>Korea Astronomy Observatory, Taejon 305-348, KOREA*E-mail: bgpark@boao.re.kr*<sup>2</sup>SEES, Seoul National University, Seoul 151-742, KOREA*E-mail: sungh@astro.snu.ac.kr*<sup>3</sup>Department of Earth Science Education, Kyungpook National University, Taegu 702-701, KOREA*E-mail: yhkang@knu.ac.kr**(Received Nov. 20, 2001; Accepted Dec. 03, 2001)*

## ABSTRACT

*UBVRI* and  $H\alpha$  photometry has been performed for the open cluster NGC 6531. A total of 56 bright main sequence (MS) members were selected from their positions in photometric diagrams. We also classified 7 pre-main sequence (PMS) stars and 6 PMS candidates with  $H\alpha$  emission from  $H\alpha$  photometry. We determined a reddening of  $< E(B - V) > = 0.29 \pm 0.03$  and a distance modulus of  $V_0 - M_V = 10.5$  for the cluster. From the comparison of our photometric results to theoretical evolution models, we derived a MS turnoff age of 7.5 Myr and a PMS age spread of  $\sim 4$  Myr. The IMF slope  $\Gamma$ , calculated in the mass range of  $0.45 \leq \log m \leq 1.35$  is a steep value of  $\Gamma = -1.8 \pm 0.6$ .

*Key words* : open clusters and associations: individual (NGC 6531) – stars: pre-main sequence

## I. INTRODUCTION

Membership determination in an open cluster can be divided into two categories. First, main sequence (MS) stars are easy to be selected because they form a well defined zero-age main sequence (ZAMS) in the photometric diagrams. Their brightness is suitable for proper motion study and spectroscopic observation to classify spectral types if they were sufficiently near. For low mass faint members, it is quite difficult to discriminate member stars from surrounding field stars so that most studies adopt statistical approach to compare the number density of stars in the reference field and cluster field.

In the case of a young open cluster, low-mass stars are still in the contraction phase and their positions in the photometric diagrams are usually crowded with foreground red stars and reddened background stars. The second category of membership assignment is to select these pre-main sequence (PMS) members. Since PMS stars can be identified by their strong Balmer line emission, strongest at  $H\alpha$ , or X-ray emission (Neuhäuser 1997), they can be selected either by  $H\alpha$  photometry or X-ray observation, or both.

Since Sung, Bessell, & Lee (1997) successfully selected the PMS members in the open cluster NGC 2264, CCD  $H\alpha$  photometry has been the most useful method for the selection of low-mass PMS stars with  $H\alpha$  emission in a young open cluster. However,  $H\alpha$  emission from a PMS star is related with a circumstellar disk and is weakened with the age of the PMS star. Therefore, there is a limit in cluster age to which the  $H\alpha$  photometry can be applied.

The young open cluster NGC 6531 (M21) is located

in the Galactic disk near the Sagittarius star forming region. The cluster is near to the nebula NGC 6514 (the Trifid nebula), but it is known that it is not associated with any nebulosity and the interstellar reddening is low and homogeneous (Forbes 1996). Although the cluster is relatively near ( $d = 1.3 kpc$ , Johnson et al. 1961), and has many early B-type stars, it has not been studied in detail. Previous photoelectric observations are focused on the bright MS stars only (Hoag et al. 1961; Forbes 1996) and faint stars are observed by photographic photometry (Zug 1933; Hoag et al. 1961; Forbes 1996). Although there are a few bright members whose MK class is determined, membership assignment is mainly done by stellar positions in the photometric diagrams even to the regions of ambiguity caused by contamination of field stars. The age of the cluster is moderately young (8 Myr, Forbes 1996).

In this study, we try to select member stars of NGC 6531 using  $H\alpha$  photometry. We also determine the characteristics of the cluster such as interstellar reddening, distance, age and age spread, and the initial mass function (IMF). In Section II, we describe the observation and data reduction. The reddening and distance to the cluster is determined in Section III, where membership assignment is also performed. In Section IV, the H-R diagram is constructed and the individual age and masses of member stars are derived from adopted theoretical evolution models, followed by the discussion of the IMF. Section V summarizes the primary results.

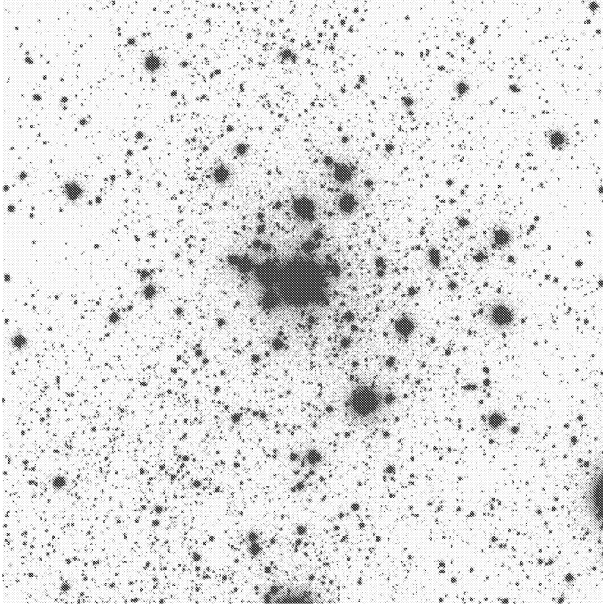
## II. OBSERVATION AND DATA REDUCTION

*UBVRI* and  $H\alpha$  CCD photometry of NGC 6531 was performed on June 25, 1997 at Siding Spring Observatory with the 1 m telescope (f/8) and a SITe 2048  $\times$

**Table 1.** Photometric data

Id.	$\alpha_{2000}$	$\delta_{2000}$	$V$	$V-I$	$B-V$	$U-B$	$R-H\alpha$	$\epsilon_V$	$\epsilon_{V-I}$	$\epsilon_{B-V}$	$\epsilon_{U-B}$	$\epsilon_{R-H\alpha}$	$n_{obs}$
1	18:03:27.3	-22:37:56	16.376	1.599	1.146	...	-4.743	0.012	0.013	0.019	...	0.020	2 2 1 1
2	18:03:27.3	-22:39:17	12.659	0.326	0.183	...	-4.956	0.001	0.001	0.001	...	0.007	2 2 2 2
3	18:03:27.3	-22:39:13	15.495	...	3.300	...	...	0.107	...	0.330	...	...	2 1
4	18:03:27.5	-22:38:58	12.460	1.176	0.837	0.293	-4.773	0.008	0.012	0.008	0.010	0.014	2 1 2 2 1
5	18:03:27.5	-22:38:55	15.223	...	4.226	...	...	0.116	...	0.324	...	...	2 1

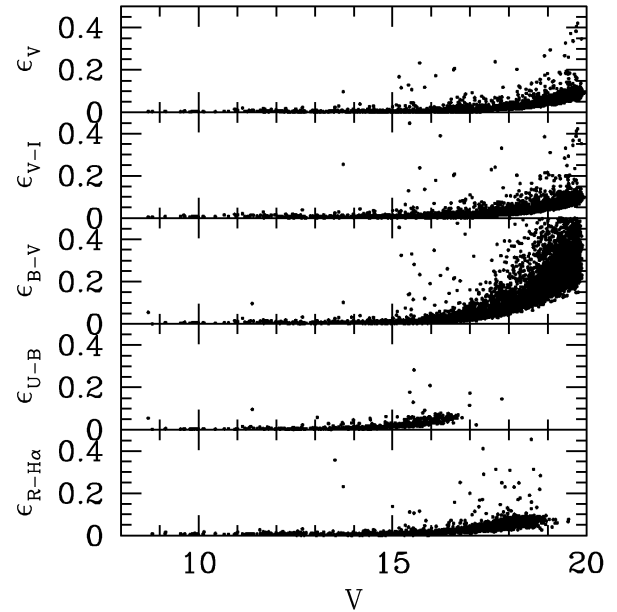
Note. — Units of right ascension are hours, minutes, and seconds, and units of declination are degrees, arcminutes, and arcseconds. Table 1 in its entire form is available by email request to [bqpark@boao.re.kr](mailto:bqpark@boao.re.kr). A portion is shown here for guidance regarding its form and content.

**Fig. 1.**— A grayscale map of the long-exposure  $V$  image of the observed region. The brightest star near center is HD 164863. North is up and east is to the left.

2048 CCD (pixel size  $24\mu$ ). The scale is  $0''.602/\text{pixel}$ , giving  $20'.5$  on a side. The central wavelength and band width of the  $H\alpha$  filter is  $6563\text{\AA}$  and  $55\text{\AA}$ , respectively. The coordinate of the image center is  $\alpha = 18^h 4^m 11^s.9$ ,  $\delta = -22^\circ 30' 1''$  (J2000.0).

Exposure times for each filter are ( $60^s, 600^s$ ) for  $U$ , ( $10^s, 300^s$ ) for  $B$ , ( $5^s, 120^s$ ) for  $V$ , ( $5^s, 90^s$ ) for  $R$ , ( $5^s, 60^s$ ) for  $I$ , and ( $30^s, 600^s$ ) for  $H\alpha$ , respectively. Two stars (HD 164844, 164863) were saturated in the short exposure  $V$  image and we used the existing photometric data (Forbes 1996, Hoag et al. 1961) after compensating zero point differences. The seeing was between  $2''$  and  $3''$ .

Each image was preprocessed by bias subtraction and flat fielding using the IRAF/CCDRED package. Instrumental magnitudes were obtained by point spread function fitting using the IRAF/DAOPHOT package.

**Fig. 2.**— Photometric errors in magnitude and color vs.  $V$  magnitude.

We transformed instrumental magnitudes to the standard system by deriving primary extinction coefficients and zero points (see Sung, Chun & Bessell 2000 for details) and adopting mean values of secondary extinction coefficients and transformation coefficients (Sung & Bessell 2000). For the  $H\alpha$  filter, we derived primary extinction coefficients only to derive extinction-free magnitudes. In order to discriminate PMS stars with  $H\alpha$  emission from normal MS stars, we used the relation for MS stars determined by Sung, Bessell, & Lee (1997).

Table 1 lists the running number,  $\alpha$ ,  $\delta$  (J2000.0), the weighted mean values of magnitude and colors with errors and the number of observations for 997 stars brighter than  $V = 17^m$ . We show a grayscale map of the long-exposure  $V$  image of the region in Fig. 1.

The errors in magnitude and color are plotted against  $V$  magnitude in Fig. 2. The  $UBV$  magnitude and col-

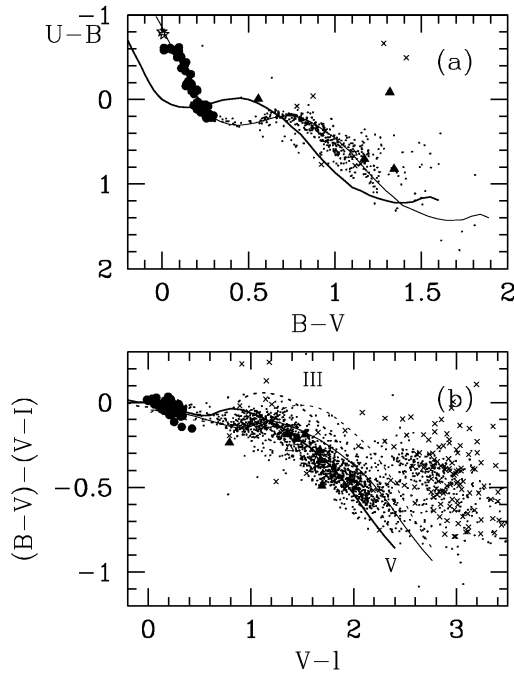


**Fig. 3.**— Color-color diagrams. The ZAMS relation for main sequence stars (V: solid line) and that for giant stars (III: dotted line) brighter than  $V = 18^m$  are shown. Thick lines are for the same relations but reddened by  $E(B-V) = 0.29$ . The symbols represent: filled circles – bright members, dots – non-member stars, small crosses – stars with poor photometric quality ( $\epsilon \geq 0.1$  mag), stars – data from photoelectric photometry of previous investigators, filled triangles – PMS stars, and open triangles – PMS candidates.

ors of stars brighter than  $V = 14$  mag from this study are compared with previous photoelectric photometry by Hoag et al. (1961) and Forbes (1996). The differences are in the sense other study minus those from this study. In the comparison, we exclude stars with differences greater than twice the standard deviation to derive the final differences and standard deviations. The differences are  $-0.032 \pm 0.018$  for  $\Delta V$ ,  $0.015 \pm 0.013$  for  $\Delta(B-V)$ , and  $0.039 \pm 0.019$  for  $\Delta(U-B)$  with Hoag et al. (1961) and  $-0.057 \pm 0.041$  for  $\Delta V$ ,  $0.007 \pm 0.009$  for  $\Delta(B-V)$ , and  $0.037 \pm 0.022$  for  $\Delta(U-B)$  with Forbes (1996). The photoelectric measurements agree well with our data in  $B-V$ , but show somewhat large differences in  $V$  and  $U-B$ .

### III. PHOTOMETRIC DIAGRAMS AND MEMBERSHIP SELECTION

#### (a) Reddening and Distance

We present the color-color diagrams in Fig. 3. Thick lines and thin lines are the reddened and unreddened ZAMS relations from Sung & Bessell (1999), respectively. In Fig 3b, solid lines indicate MS loci and dot-

ted lines the giant loci. The star symbols represent bright stars whose colors are adopted from photoelectric photometry. Other symbols are, filled circles: MS members, filled triangles: PMS stars with  $H\alpha$  emission, open triangles: PMS candidates, dots: non-member stars, small crosses: stars with poor photometric quality ( $\epsilon \geq 0.1$ ). The membership selection is described in the next section. In Fig. 3a, early type stars show a well-defined MS band which implies the differential reddening across the cluster is small. The UV-excess from PMS stars is not so strong except one star. In Fig 3b, PMS stars with  $H\alpha$  emission are indistinguishable from MS stars, unlike the same type of stars in NGC 2264 (Park et al. 2000) and NGC 2244 (Park & Sung 2002).

We adopt the mean color excess ratio of  $E(U-B)/E(B-V) = 0.72$  and calculate the mean reddening to the cluster as  $\langle E(B-V) \rangle = 0.29 \pm 0.03$  from individual reddening values for 45 member stars brighter than  $V = 13$  mag. The individual reddening value ranges from 0.22 to 0.34. Stars located north-eastern part of the cluster show larger reddening value. The mean reddening value determined in this study is in good agreement with previous ones (0.28, Hoag et al. 1961; 0.3, Forbes 1996). By adopting the value of the total to selective extinction ratio,  $R_V = 3.1$  and the reddening value determined above, we calculate the distance to the individual stars from the  $V$  versus  $B-V$  color-magnitude diagram shown in Fig. 4b. The mean distance calculated from 34 stars whose distance values are between 10.0 and 10.6 is  $10.3 \pm 0.1$ . Considering the existence of binaries and the higher luminosity from evolved massive stars, this value would be an underestimation of the true mean distance to the cluster. Therefore, we analyze the histogram distribution of the distance moduli of individual stars and take the value at the falling edge of the histogram. As a result, we adopt the distance modulus of the cluster as  $V_0 - M_V = 10.5$  (1.3 kpc). This value is in good agreement with previous determinations (10.5, Janes & Adler 1982; Forbes 1996).

We show the color-magnitude diagrams of NGC 6531 in Fig. 4. While most MS members distribute well along the MS locus, PMS stars with  $H\alpha$  emission are located above the ZAMS in Fig. 4a and 4b, except some stars near the ZAMS. The low luminosity of these stars may be explained by the same way as the two faint PMS stars in NGC 2244 (Park & Sung 2002). In Fig. 4c, we can notice the UV-excess of the PMS stars with  $H\alpha$  emission is not remarkable except one star. The PMS stars with  $H\alpha$  emission are clearly identified by their large value of  $R-H\alpha$  in Fig. 4d, along with one possible Herbig Ae star.

#### (b) Membership Selection

##### i) MS members

As an attempt to assign the cluster members, Forbes (1996) lists probable members selected on the basis of

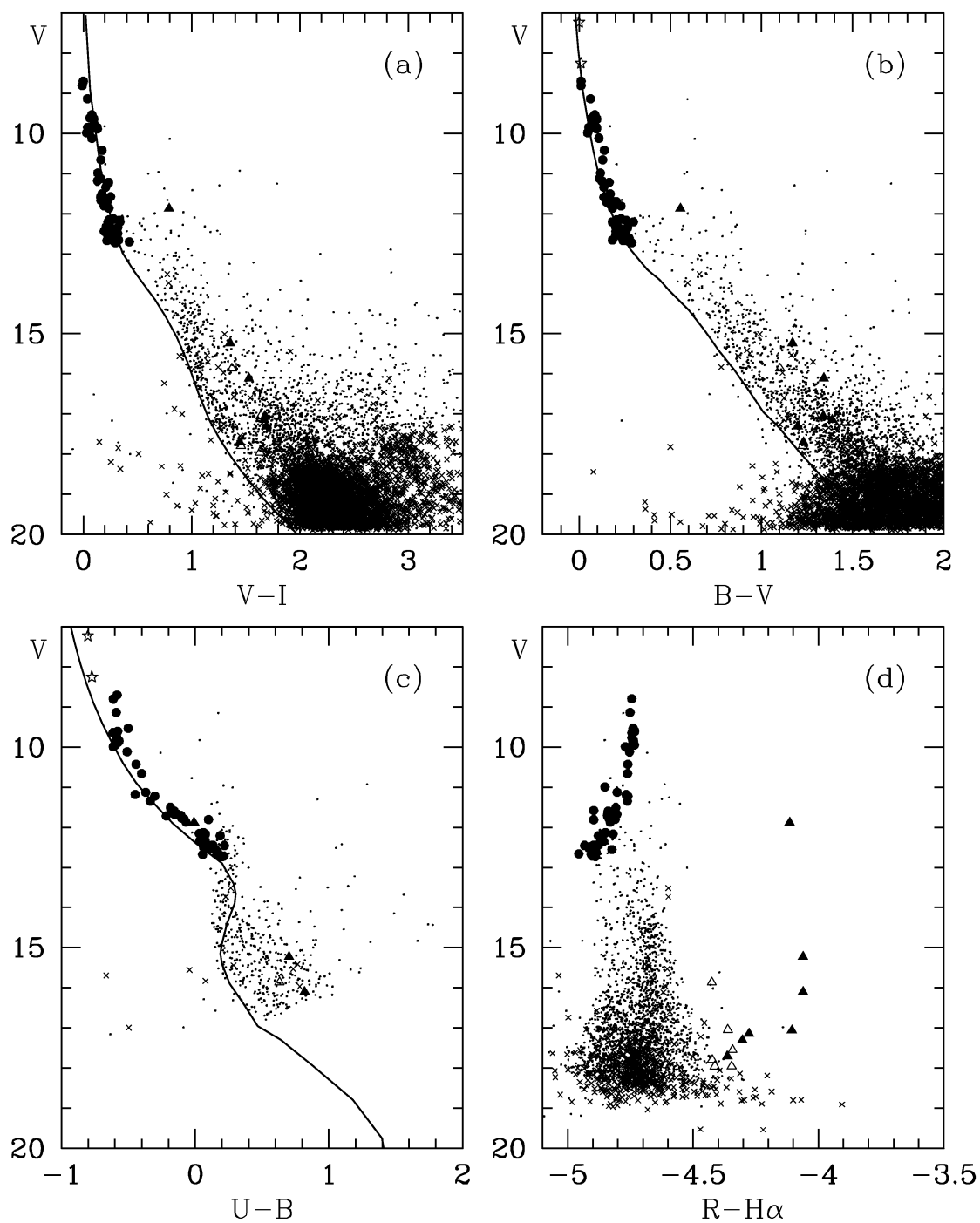


**Fig. 4.**— Color-magnitude diagrams. The lines represent the reddened ZAMS relations. Symbols are the same as in Fig. 3.



**Table 2.** PMS and PMS candidate stars in NGC 6531

Id.	$V$	$V-I$	$B-V$	$U-B$	$R-H\alpha$	$\epsilon_V$	$\epsilon_{V-I}$	$\epsilon_{B-V}$	$\epsilon_{U-B}$	$\epsilon_{R-H\alpha}$	$n_{obs}$	Remark
153	15.227	1.356	1.170	0.702	-4.061	0.006	0.007	0.008	0.027	0.026	2 2 2 1 2	PMS
230	11.878	0.792	0.556	-0.008	-4.114	0.009	0.013	0.012	0.007	0.008	2 2 2 2 1	Herbig Ae?
310	16.105	1.529	1.342	0.819	-4.061	0.005	0.005	0.011	0.067	0.013	2 2 1 1 1	PMS
622	15.861	1.373	1.103	0.631	-4.425	0.003	0.017	0.034	0.055	0.070	2 2 2 1 1	PMS cand.
1001	17.050	1.639	1.295	...	-4.361	0.010	0.011	0.024	...	0.025	2 2 1	1 PMS cand.
1002	17.146	1.671	1.389	...	-4.277	0.006	0.006	0.027	...	0.025	2 2 1	1 PMS
1003	17.797	1.457	1.226	...	-4.424	0.018	0.027	0.046	...	0.056	1 1 1	1 PMS cand.
1004	17.547	2.093	1.474	...	-4.342	0.018	0.019	0.053	...	0.031	1 1 1	1 PMS cand.
1005	17.962	2.091	1.666	...	-4.346	0.019	0.019	0.072	...	0.046	1 1 1	1 PMS cand.
1006	17.051	1.678	1.339	...	-4.106	0.003	0.006	0.020	...	0.021	2 2 1	1 PMS
1007	17.701	1.445	1.231	...	-4.363	0.018	0.050	0.053	...	0.062	1 1 1	1 PMS
1008	17.306	1.691	1.199	...	-4.303	0.024	0.031	0.054	...	0.038	1 1 1	1 PMS
1009	17.952	1.632	1.558	...	-4.413	0.018	0.018	0.056	...	0.051	1 1 1	1 PMS cand.

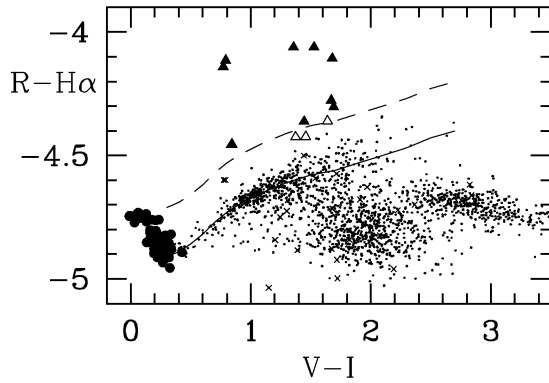


**Fig. 5.**— The  $R-H\alpha$  vs.  $V-I$  diagram. The solid line represents the MS relation adopted from Sung et al. (1997), but shifted by  $E(V-I) = 0^m.13$  and the dashed line shows the selection limit of  $H\alpha$  emission stars. Symbols are the same as in Fig. 3.

their positions in the photometric diagrams in his tables 1 and 2. Forbes(1996)'s probable member stars show  $V$  magnitude down to 16 mag and  $B-V$  range of 0 - 1.24. However, as the cluster lies very close to the Galactic disk ( $b = -0^\circ.44$ ), there must be many field stars indistinguishable from cluster members, as we see in Fig. 4b. Therefore, we only refer to his estimation of upper limit on the number of the member stars from statistical analysis,  $105 \pm 11$  to the limiting magnitude of  $V = 15.5$ .

For the selection of MS members in the cluster, we constrain ourselves to the stars with  $V \leq 13$  and  $B-V \leq 0.3$  only, to minimize possible contamination of field stars. Further selection criteria for the MS members are the positions in the  $V$  versus  $V-I$ ,  $U-B$  versus  $B-V$ , and  $(B-V) - (V-I)$  versus  $V-I$  color-magnitude and color-color diagrams. The resulting number of bright member stars is 56, down to  $V \sim 13$  mag and bluer than  $B-V = 0.3$ .

## ii) PMS members

For photometric membership selection of low mass PMS stars with  $H\alpha$  emission, CCD  $H\alpha$  photometry has been proved to be the most useful method (Sung, Bessell & Lee 1997). Although  $H\alpha$  emission from a PMS star is likely to be ceased for stars of mass  $\sim 2M_\odot$  and age  $\geq 2$  Myr due to the destruction of accretion disk of such stars (Park & Sung 2002),  $H\alpha$  photometry can still be a good guideline to discriminate a PMS star with  $H\alpha$  emission from field stars.

In order to select PMS stars with  $H\alpha$  emission in NGC 6531, we use the standard relation between  $R-H\alpha$  and  $V-I$  for the field stars toward NGC 2264 determined by Sung, Bessell, & Lee (1997, Table 3). The reason for this is first, we use the same telescope, CCD camera, and  $H\alpha$  filter as those used by them, and second, the direction toward NGC 2264 is almost extinction-free to make a reliable relation between the two color indices. We deredden the standard relation for the foreground MS stars by compensating  $E(B-V) = 0.1$  estimated from the color-color diagram shown in Fig. 3.

We tentatively assign a star as a PMS star if its value of  $\Delta(R-H\alpha) [\equiv (R-H\alpha)_{star} - (R-H\alpha)_{MS}]$  is greater than 0.2 mag and as a PMS candidate if  $0^m.1 \leq \Delta(R-H\alpha) \leq 0^m.2$ . We show the distribution of stars in  $R-H\alpha$  versus  $V-I$  diagram in Fig. 5. In Fig. 5, we show the relation for the MS stars as solid line and the selection limit to discriminate PMS stars as dashed line. As a result, we selected one possible Herbig Ae star, 6 PMS stars with  $H\alpha$  emission, and 6 PMS candidates.

Although we have selected 13 PMS stars with  $H\alpha$  emission, we believe that there should be more PMS stars undetectable by  $H\alpha$  photometry. If we assume the estimation of total member stars by Forbes (1996), there should exist about 40 to 60 PMS stars brighter than  $V = 15.5$  in the cluster. On the other hand, there are only two stars which fulfill the brightness limit in

our PMS star list. Therefore, we can conclude the  $H\alpha$  emission from most of the PMS stars is not strong enough to be detected by  $H\alpha$  photometry. Considering the cluster age is around 8 Myr, the accretion disk around PMS stars more massive than  $1 M_{\odot}$  may have been destructed (see Haisch, Lada, & Lada 2001). In this case, we could try to resolve the PMS stars in NGC 6531 by X-ray observation, for the X-ray emission from PMS stars becomes stronger as disk activity weakens (Neuhäuser 1997).

Therefore, the current result of  $H\alpha$  photometry is only meaningful in a sense that we can identify PMS stars with strong  $H\alpha$  emission individually, not statistically. The number of detected PMS stars with  $H\alpha$  emission is not significant for subsequent analysis of PMS age, age spread, and the IMF. PMS stars and PMS candidates of NGC 6531 are listed in Table 2.

#### IV. AGE AND THE IMF

##### (a) H-R Diagram

We dereddened bright MS stars by estimating individual reddening values from  $U - B$  versus  $B - V$  diagram. For other stars, we interpolated their reddening values according to their relative spatial positions or adopted a mean reddening value. The temperature calibration of Sung & Lee (1995) and the bolometric correction scales of Balona (1994) were adopted to derive luminosity and effective temperature of the MS stars. For low mass PMS stars, temperature and bolometric correction scale relations from Bessell (1995) were used for stars redder than  $V - I = 1.3$  and for bluer stars, relations from Bessell, Castelli, & Plez (1998) were adopted.

We show the H-R diagram of NGC 6531 using the adopted relations in Fig. 6. The stellar evolution models of the Geneva group (Schaller et al. 1992) and the PMS evolution models by Swenson et al. (1994, hereafter SFRI, their model F) are superposed.

##### (b) Age and Age Spread

We can estimate the MS turnoff age of the cluster from the H-R diagram shown in Fig. 6. Most bright stars form a distinct sequence along the ZAMS, and some stars are located above ZAMS. The higher luminosity of these stars is because they are spectroscopic binaries, and therefore is not the result of the evolutionary effect. We fit the cluster MS turnoff age by fitting the age of the most massive star by the Geneva isochrone of 7.5 Myr which is shown in the figure.

Amongst 13 PMS stars in the cluster, we can estimate the ages of 7 stars. By fitting the PMS evolution tracks of SFRI and D'Antona & Mazzitelli (1994, hereafter DM94, CM convection and Alexander opacities models) to the PMS stars, we estimate the mean age of 3.5 Myr for SFRI and 3 Myr for DM94, respectively.

Although there are only small number of PMS stars

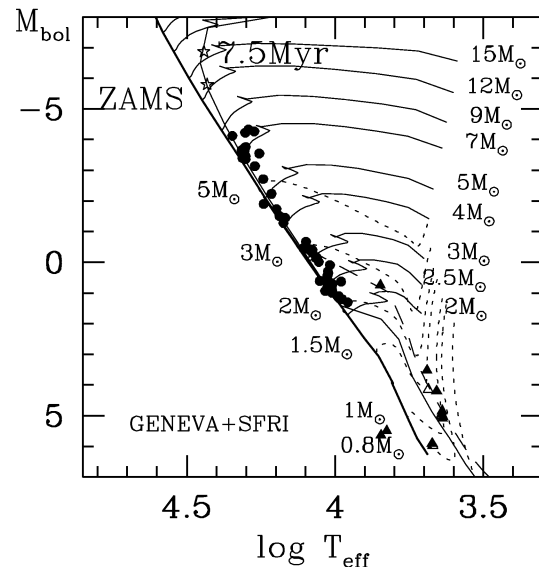


**Fig. 6.**— The H-R diagram of NGC 6531. The thick solid line represents the ZAMS of Schaller et al. (1992). The thin solid lines with mass to the right are the stellar evolution tracks of Schaller et al., while the dotted lines with mass to the left are the PMS evolution tracks by Swenson et al. (1994). The thin line intersecting the evolutionary tracks represents an isochrone of 7.5 Myr, and dashed line is a PMS isochrone of 3 Myr. Symbols are the same as in Fig. 3.

in the statistics, the mean PMS age can give a clue to the cluster formation time, i.e., the age spread of the cluster. We estimate the MS turnoff age of 7.5 Myr, and the age spread of 4 Myr to NGC 6531.

##### (c) Initial Mass Function

The masses of member stars are determined from the Geneva models for MS stars and from the SFRI and DM94 models for PMS stars and PMS candidates. We constructed the IMF for the mass range  $-0.3 \leq \log m \leq 1.5$ , with mass bins of 0.3 dex. The IMF calculations were done twice with the same bin size, but shifted by 0.15 in  $\log m$  in order to smooth out possible binning effects. The resulting IMF is shown in Fig. 7.

In Fig. 7, symbols are IMF for NGC 6531 with error bar, thick line represents the slope of the IMF, and thin line is the field star IMF of the solar neighborhood (Scalo 1986). Comparing the IMF of NGC 6531 with that of the solar neighborhood, the two IMFs show similar trend down to  $\log m \sim 0.5$ .

The slope of the IMF,  $\Gamma \equiv d \log \xi(\log m) / d \log m$ , is  $\Gamma = -1.8 \pm 0.6$ , in the range of  $0.45 \leq \log m \leq 1.35$ . This value is somewhat steeper than  $\Gamma = -1.29 \pm 0.17$  derived by Forbes (1996) from the luminosity function of NGC 6531 by photographic photometry. The steep IMF slope of NGC 6531 is comparable to that of NGC 2264 derived by Park et al. (2000).

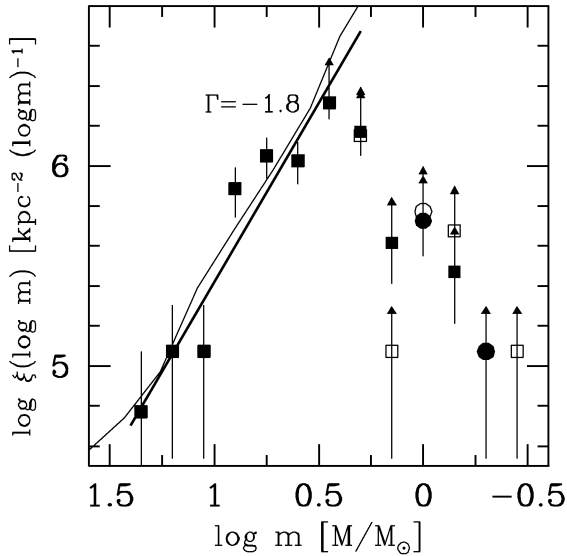


**Fig. 7.**— The IMF of NGC 6531. Dots and squares represent the IMF binned by 0.3 in  $\log m$ , but shifted by 0.15 in  $\log m$  to avoid possible binning effects. Closed symbols are for the models Geneva and SFRI, and open symbols are for the models Geneva and DM94, respectively. The thin solid line is the field star IMF of the solar neighborhood by Scalo (1986) after arbitrary scaling. The thick solid line represents the slope of the IMF and we obtained the IMF slope,  $\Gamma = -1.8 \pm 0.6$  in the range  $0.45 \leq \log m \leq 1.35$ . The arrow heads represent the incompleteness of data and the error bars are based on  $\pm\sqrt{N}$ .

## V. SUMMARY

We performed a *UBVRI* and  $H\alpha$  CCD photometry of the young open cluster NGC 6531. We selected 56 MS members brighter than  $V = 13$  mag from their positions in the *UBVI* photometric diagrams. The mean reddening determined from 45 member stars brighter than  $V = 13$  mag was  $E(B - V) = 0.29 \pm 0.03$  by adopting a mean color excess ratio of  $E(U - B)/E(B - V) = 0.72$ . The distance modulus was derived as  $V_0 - M_V = 10.5$  ( $1.3 \text{ kpc}$ ) with the value of total to selective extinction ratio  $R_V = 3.1$ . We also selected 7 PMS stars with strong  $H\alpha$  emission and 6 PMS candidates with weak  $H\alpha$  emission from  $R - I$  versus  $V - I$  color-color diagram.

We derived the MS turnoff age of the cluster as 7.5 Myr by adopting the Geneva evolution models for 56 MS stars. The PMS age of the cluster was derived as 3 Myr using the SFRI model and 3.5 Myr using the DM94 model with relatively small number of seven PMS stars. From these two age estimations, we attributed the age spread of the cluster as  $\sim 4$  Myr.

Since there may exist 40 to 60 low mass PMS stars in the cluster, the current sample of PMS stars is too small to be meaningful for statistical analysis of the PMS characteristics of the cluster. The IMF of the cluster shows similar trend as the field star IMF of the solar neighborhood in the mass range down to  $\log m \simeq 0.5$ . The slope of the IMF,  $\Gamma$  was calculated as  $\Gamma = -1.8 \pm 0.6$  in the mass range of  $0.45 \leq \log m \leq 1.35$ .

HS wishes to thank the staff of the Research School of Astronomy and Astrophysics for the use of the 40 inch telescope and facilities at Siding Spring Observatory. This work was partially supported by the Kyungpook National University Research Fund, 2001 and grant No. R01-2001-00026 from the Korea Science and Engineering Foundation.

## REFERENCES

- Balona, L.A. 1994, MNRAS, 268, 119
- Bessell, M.S. 1995, in *The Bottom of the Main Sequence and Beyond*, ed. C. Tinney (Berlin: Springer), 123
- Bessell, M.S., Castelli, F., & Plez, B. 1998, A&A, 333, 231
- D'Antona, F., & Mazzitelli, I. 1994, ApJS, 90, 467 (DM94)
- Forbes, D. 1996, AJ, 112, 1073
- Haisch, K.E.Jr., Lada, E.A., & Lada, C.J. 2001, ApJ, 553, L153
- Hoag, A.A., Johnson, H.L., Iriarte, B., Mitchell, R.I., Hallam, K.L., & Sharpless, S. 1961, Pub. U.S. Naval Obs., 17, 343
- Janes, K., & Adler, D. 1982, ApJS, 49, 425
- Johnson, H.L., Hoag, A.A., Iriarte, B., Mitchell, R.I., & Hallam, K.L. 1961, Lowell Obs. Bull., 5, 133
- Neuhäuser, R. 1997, Science, 276, 1363
- Park, B.-G., & Sung, H. 2002, AJ, in press (Feb. issue)
- Park, B.-G., Sung, H., Bessell, M.S., & Kang, Y.H. 2000, AJ, 120, 894
- Scalo, J. 1986, Fund. Cosmic Phys., 11, 1
- Schaller, G., Schaerer, D., Meynet, G., & Maeder, A. 1992, A&AS, 96, 269 (Geneva)
- Sung, H., & Bessell, M.S. 1999, MNRAS, 306, 361
- Sung, H., & Bessell, M.S. 2000, Pub. Ast. Soc. Australia, 17, 244
- Sung, H., Bessell, M.S., & Lee, S.-W. 1997, AJ, 114, 2644
- Sung, H., Chun, M.-Y., & Bessell, M.S. 2000, AJ, 120, 333
- Sung, H., & Lee, S.-W. 1995, JKAS, 28, 119
- Swenson, F.J., Faulkner, J., Rodgers, F.J., & Iglesias, C.A. 1994, ApJ, 425, 286 (SFRI)
- Zug, R.S. 1933, Lick Obs. Bull. 454, 119